

AperTO - Archivio Istituzionale Open Access dell'Università di Torino

**Gene expression in vessel-associated cells upon xylem embolism repair in *Vitis vinifera* L. petioles.**

**This is the author's manuscript**

*Original Citation:*

*Availability:*

This version is available <http://hdl.handle.net/2318/144209> since 2017-05-16T10:51:58Z

*Published version:*

DOI:10.1007/s00425-013-2017-7

*Terms of use:*

Open Access

Anyone can freely access the full text of works made available as "Open Access". Works made available under a Creative Commons license can be used according to the terms and conditions of said license. Use of all other works requires consent of the right holder (author or publisher) if not exempted from copyright protection by the applicable law.

(Article begins on next page)



# UNIVERSITÀ DEGLI STUDI DI TORINO

1  
2  
3  
4  
5  
6  
7  
8

*The final publication is available at Springer*  
*via <http://dx.doi.org/10.1007/s00425-013-2017-7>*

9

10 **Journal: PLANTA Springer**

11

12 **Title: Gene expression in vessel-associated cells upon xylem embolism repair in**  
13 ***Vitis vinifera* L. petioles**

14

15 **Authors:** Walter Chitarra<sup>1</sup>, Raffaella Balestrini<sup>2</sup>, Marco Vitali<sup>1</sup>, Chiara Pagliarani<sup>1\*</sup>,  
16 Irene Perrone<sup>1§</sup>, Andrea Schubert<sup>1</sup>, Claudio Lovisolo<sup>1,3</sup>

17

18 <sup>1</sup> University of Turin, Department of Agricultural, Forest and Food Sciences (DISAFA),  
19 Via Leonardo da Vinci 44, I-10095 Grugliasco (TO), Italy.

20 <sup>2</sup> Plant Protection Institute, National Research Council (IPP-CNR), Torino unit, Viale  
21 Mattioli 25, I-10125 Torino, Italy

22 <sup>3</sup> Plant Virology Institute, National Research Council (IVV-CNR), Grugliasco unit, Via  
23 Leonardo da Vinci 44, I-10095 Grugliasco (TO), Italy.

24

25 **\*Author for correspondence:**

26 Chiara Pagliarani

27 Telephone: +39 011 670 8645

28 Fax: +39 011 670 8658

29 e-mail: chiara.pagliarani@unito.it

30

31 <sup>§</sup>presently at Department of Forest Genetics and Plant Physiology, Swedish University  
32 of Agricultural Sciences (SLU), SE-901 87 Umeå, Sweden.

33

34

35 **Abstract**

36 In this work, the involvement of vessel-associated cells in embolism recovery was  
37 investigated by studying leaf petiole hydraulics and expression profiles of aquaporins  
38 and genes related to sugar metabolism.

39 Two different stress treatments were imposed onto grapevines to induce xylem  
40 embolism: one involved a pressure collar applied to the stems, while the other consisted  
41 of water deprivation (drought). Embolism formation and repair were monitored during  
42 stress application and release (recovery). At the same time, stomatal conductance ( $g_s$ ),  
43 leaf water potential ( $\Psi_{\text{leaf}}$ ), and leaf abscisic acid (ABA) concentration were measured.  
44 For each treatment, gene transcript levels were assessed on vessel-associated cells  
45 (isolated from leaf petioles by laser microdissection technique) and whole petioles.

46 Both treatments induced severe xylem embolism formation and drops in  $g_s$  and  $\Psi_{\text{leaf}}$  at a  
47 lesser degree and with faster recovery in the case of application of the pressure collar.  
48 Leaf ABA concentration only increased upon drought and subsequent recovery.  
49 Transcripts linked to sugar mobilisation (encoding a  $\beta$ -amylase and a glucose-6-P  
50 transporter) were over-expressed upon stress or recovery both in vessel-associated cells  
51 and whole petioles. However, two aquaporin genes (*VvPIP2;1* and *VvPIP2;4N*) were  
52 activated upon stress or recovery only in vessel-associated cells, suggesting a specific  
53 effect on embolism refilling. Furthermore, the latter gene was only activated upon  
54 drought and subsequent recovery, suggesting that either severe water stress or ABA are  
55 required for its regulation.

56

57 **Keywords:** Aquaporins, Drought, Grapevine, Laser microdissection, Pressure collar,  
58 Sugar metabolism.

59

60 **Abbreviations:** ABA (Abscisic acid), IRR (Irrigated), WS (Water stress), RWS  
61 (Recovery from water stress), PC (Pressure collar), RPC (Recovery from pressure  
62 collar), HCFM (Hydraulic Conductance Flow Meter), LMD (Laser MicroDissection),  
63 RT-qPCR (Quantitative Real-Time PCR), VACs (Vessel Associated Cells).

64

65 **Introduction**

66

67 Vascular plants have evolved a long-distance transport system for water and minerals  
68 through non-living xylem vessels. Long distance transport is driven by tension, as  
69 postulated by the Cohesion-Tension theory (Tyree 2003) and further confirmed by  
70 direct measurements of negative pressures in xylem (Angeles et al. 2004). Under high  
71 tension (e.g., upon drought stress), water is metastable and, when gas-filled, xylem  
72 vessels may become disrupted by breakage of water column continuity (cavitation), thus  
73 causing embolism that drastically reduces the hydraulic conductance of xylem (in  
74 grapevine, Schultz and Matthews 1988; Lovisolo and Schubert 1998; Tramontini et al.  
75 2013). However, many aspects concerning the biophysics of embolism formation in  
76 plants remain unclear (Clearwater and Goldstein 2005). Several studies suggested that  
77 xylem cavitation is caused by environmental stress, such as drought (e.g., Tyree et al.  
78 1994; Davis et al. 2002) and freezing temperatures (e.g., Just and Sauter 1991; Nardini  
79 et al. 2000; Sakr et al. 2003). Nevertheless, cavitation is also a daily cyclical  
80 phenomenon occurring even in well-watered plants (Holbrook et al. 2001; Lovisolo et  
81 al. 2008; Zufferey et al. 2011).

82 Xylem embolisms can be refilled (recover) when xylem tension drops to values close to  
83 zero. However, embolism recovery takes place also upon tension, and plant metabolism  
84 plays an essential role in these conditions, as demonstrated by the effect of metabolic  
85 inhibitors (Salleo et al. 1996, 2004; Lovisolo and Schubert 2006). Furthermore,  
86 modifications of transcriptional profiles observed upon embolism recovery (Brodersen  
87 et al. 2010, 2013; Secchi and Zwieniecki 2010, 2011; Perrone et al. 2012b) suggest that  
88 plants can mount specific responses to xylem embolism. Different models have been  
89 proposed to explain how plants induce an embolism-refilling process, most of which  
90 include key roles for living parenchyma cells surrounding xylem vessels (Vessel-

91 Associated Cells: VACs). In these cells a decrease in starch content and an increase in  
92 sucrose concentration are observed upon refilling (Salleo et al. 2009; Secchi and  
93 Zwieniecki 2010, Nardini et al. 2011). Sucrose is probably translocated to adjacent  
94 embolised vessels (Holbrook and Zwieniecki 1999; Tyree et al. 1999; Salleo et al. 2004;  
95 Secchi et al. 2012), where it helps to establish an osmotic gradient that draws water into  
96 the emboli by aquaporin-mediated transport. The involvement of starch hydrolysis and  
97 water transport facilitators in the refilling process is supported by upregulation of genes  
98 encoding  $\beta$ -amylases and plasma membrane intrinsic proteins (PIPs) in recovering  
99 shoots of *Juglans regia*, *Populus trichocarpa*, and *Vitis vinifera* (Sakr et al. 2003;  
100 Kaldenhoff et al. 2008; Secchi and Zwieniecki 2010, 2011; Perrone et al. 2012b).

101 Besides describing the molecular processes involved, a few studies have focused on the  
102 signal transduction pathways induced by the presence of xylem embolism. Secchi et al.  
103 (2011) investigated global gene expression responses in poplar subjected to artificial  
104 cavitation, and they proposed a novel role for oxygen as a signal molecule acting in  
105 parenchyma cells and triggering xylem refilling. In previous studies (Lovisolò et al.  
106 2008; Perrone et al. 2012b), we reported high levels of ABA in petioles recovering from  
107 embolism under high transpiration conditions, and we hypothesized an active role of  
108 this hormone in triggering recovery processes. Thus, the metabolic *scenario* of  
109 embolism recovery is still debated. Moreover, although it is supposed that most of these  
110 metabolic reactions take place in VACs, this has never been proven directly due to  
111 technical difficulty of isolating these cells.

112 The Laser MicroDissection (LMD) technique is a powerful tool to isolate cell  
113 populations from heterogeneous tissues and offers the possibility of exploring transcript  
114 profiles in specific cell types. LMD has successfully been used to study gene expression  
115 in different plant tissues, such as epidermal cells, shoot meristem tissues, root cap  
116 tissues and specific cells involved in plant-microbe interactions, such as those colonised

117 by arbuscular mycorrhizal or pathogenic fungi (Balestrini et al. 2009; Gomez and  
118 Harrison 2009; Chandran et al. 2010; Giovannetti et al. 2012).

119 In this study, we induced xylem cavitation and subsequent recovery in grapevine leaf  
120 petioles using two different techniques: one involved pressure application and release to  
121 the stems, while the other consisted of water deprivation (drought) followed by  
122 irrigation. We used LMD to dissect VACs from embolised petioles, and we profiled the  
123 expression of genes involved in sugar metabolism and transport, as well as in water  
124 transport facilitation, in both VAC and whole petiole samples. We demonstrate that  
125 while some of the tested genes are activated by stress and subsequent recovery in whole  
126 petioles, some aquaporin genes are exclusively expressed in VACs, supporting the  
127 conclusion that the related proteins have a specific role in the embolism recovery  
128 process.

129

130

## 131 **Materials and methods**

132

### 133 Plant material and experimental setup

134

135 Two-year-old *Vitis vinifera* L. cv. Grenache plants [Vivai Cooperativi Rauscedo-San  
136 Giorgio della Richinvelda (PN), Italy] grafted onto *Vitis riparia* x *Vitis berlandieri*  
137 420A were grown in a glasshouse under partially controlled climate conditions. The  
138 temperature in the greenhouse was maintained in the 26–35°C range, and natural  
139 light/night cycles were followed. Maximum photosynthetic photon flux density (PPFD)  
140 ranged between 1330 and 1580  $\mu\text{mol m}^{-2} \text{s}^{-1}$ . Each plant grew in a 10-l pot filled with a  
141 substrate composed of a sandy-loam soil (pH 7.0; available P 7.9 mg kg<sup>-1</sup>; organic  
142 matter 1.37%; cation exchange capacity 4.58 meq 100 g<sup>-1</sup>)/expanded clay/peat mixture



143 (2:1:1 by weight). From budbreak (February, 10<sup>th</sup>) to the beginning of the experimental  
144 period (August 1), plants were irrigated twice a week to maintain water container  
145 capacity.

146 Treatments were applied during a period of high atmospheric evaporative water demand  
147 in August (vapour pressure deficit averaging 25 mbar bar<sup>-1</sup>). Among the 36 plants used  
148 in this study, 24 were maintained at container capacity (Lovisolo and Schubert 1998):  
149 50% of these plants were used as control (12 IRR replicate plants), and 50% were  
150 subjected to artificial cavitation, imposed using a pressure collar (PC) treatment (12  
151 replicate plants) followed by depressurisation (RPC). The remaining 12 plants were  
152 subjected to water stress (WS) treatment followed by rehydration (RWS).  
153 Measurements and tissue samples were taken on one experimental day. To allow the  
154 collection of data from a sufficient number of replicates, plants were distributed among  
155 four experimental days: in each of them, three randomly chosen IRR, three PC-RPC,  
156 and three WS-RWS plants were subjected to analysis.

157 For the PC treatment, shoots of normally irrigated plants were exposed to positive  
158 pressures, following the procedure reported by several authors (Salleo et al. 1996, 2004;  
159 Tyree et al. 1999; Secchi and Zwieniecki 2010) with minor modifications. Our system  
160 consisted of a narrow-diameter tube (diameter, 19.1 mm) sealed around the basal  
161 internode of the shoot by using a custom-built holder and allowing the application of  
162 pressure around the stem. During the experimental day, at 11:00 h, the pressure collar  
163 was connected to a gaseous N<sub>2</sub> bomb to maintain a 2.7 MPa pressure for five hours.  
164 Thereafter (at 16:00 h), the collar was removed in order to induce depressurisation and  
165 recovery.

166 For the WS treatment, irrigation was withheld for a 10-d period prior to the  
167 experimental day. This treatment induces cavitation in grapevine without producing  
168 stress-related modifications of xylem development (Schultz and Matthews 1988;

169 Lovisolo and Schubert 1998; Lovisolo et al. 2008). Water-stressed plants were  
170 rehydrated at 16:00 h of the experimental day by watering pots to container capacity.  
171 For each experimental day, one replicate plant within each treatment was used for: i)  
172 leaf gas exchange and xylem embolism analysis; ii) leaf water potential measurement  
173 and iii) petiole and leaf sampling for LMD, and for gene expression on whole petioles  
174 and ABA analysis.

175

176 Leaf gas exchange, leaf water potential and xylem embolism

177

178 Transpiration rate ( $E$ ) and stomatal conductance ( $g_s$ ) were measured on adult, non-  
179 senescing leaves well exposed to direct sunlight [PPFD (400–700 nm)  $\geq 1200 \mu\text{mol m}^{-2}$   
180  $\text{s}^{-1}$ ], using an infrared gas analyser ADC-LCPro+ system (The Analytical Development  
181 Company Ltd, Hoddesdon, UK). Measurements were taken on one leaf per plant at 30  
182 min intervals between 10:00 and 19:00 h on each experimental day, and on IRR and  
183 RWS plants also on the day after. Leaf water potential ( $\Psi_{\text{leaf}}$ ) was assessed on one  
184 transpiring leaf per plant and at each of the same time points by using a Scholander-type  
185 pressure chamber (Soil Moisture Equipment Corp., Santa Barbara, CA, USA).

186 Xylem embolism extent was measured on leaf petioles, as previously described by  
187 Lovisolo et al. (2008), using a Hydraulic Conductance Flow Meter (HCFM-XP,  
188 Dynamax Inc., Houston, TX, USA) (Tyree et al. 1995). Measurements were made at  
189 16:00 h of the experimental day for IRR, WS and PC treatments, at 19:00 h of the same  
190 day for the RPC treatment, and at 19:00 h of the following day for the RWS treatment.  
191 Briefly, one leaf petiole per plant was cut under water by bending the shoot and  
192 submerging the petiole into a water container. Embolism extent was determined by  
193 comparing the initial hydraulic conductivity ( $K_{\text{hi}}$ ) with the maximum final hydraulic  
194 conductivity ( $K_{\text{hf}}$ ) recorded after a transient water flushing designed to eject the

195 embolism from the petiole. The intensity of embolism was expressed as the percentage  
196 loss of conductivity (PLC) and calculated as  $100 * (K_{hf} - K_{hi}) / K_{hf}$ . Significant  
197 differences among treatments were determined by applying a one-way ANOVA test  
198 using the SPSS statistical software package (SPSS Inc., Cary, NC, USA, v.20).

199

200 Laser microdissection of vessel-associated cells, RT-PCR and semi-quantitative RT-  
201 PCR analyses

202

203 Two petioles per plant were collected at the same time points of PLC determination.  
204 They were cut into about 5-mm segments and immediately fixed in Farmer's solution  
205 (EAA), containing 75% (v/v) ethanol and 25% (v/v) acetic acid (Kerk et al. 2003), then  
206 stored overnight at 4°C for paraffin embedding. Farmer's solution was then removed  
207 and petiole segments were dehydrated in a graded series (30-min steps) of ice-cold  
208 ethanol (70%, 90% in sterile water and 100% [v/v] twice), followed by 100% Neoclear  
209 (Merck, Darmstadt, Germany). The petiole segments were then gradually replaced with  
210 paraffin (Paraplast plus; Sigma-Aldrich, St Louis, MO, USA), following the protocol  
211 described by Balestrini et al. (2007). Petiole sections (12 µm) were cut using a rotary  
212 microtome and transferred onto Leica RNase-free PEN foil slides (Leica Microsystem,  
213 Inc., Bensheim, Germany) with sterile double-distilled water (ddH<sub>2</sub>O, Elga LabWater,  
214 Lane End Industrial Park, UK). Sections were dried at 40°C in a warming plate, stored  
215 at 4°C, and used within 1 day.

216 A Leica AS LMD system was used to isolate cells from dried sections. Just before use,  
217 the paraffin sections were deparaffinised by Neoclear treatment for 10 min and 100%  
218 ethanol for 1 min, and then they were air-dried. The slides were placed face down on  
219 the microscope. Laser parameters for dissection of selected cells were 40-XT objective

220 at power 45–55, and speed 4. The cells from each biological replicate were  
221 subsequently collected (within one day) into a 0.5 ml RNase-free PCR tube.  
222 After collection, 50 µl of PicoPure RNA extraction buffer (Arcturus Engineering,  
223 Mountain View, CA, USA) were added to each tube, followed by incubation at 42°C  
224 for 30 min, centrifugation at 800 g for 2 min, and storage at –80°C. RNA was extracted  
225 using the PicoPure kit (Arcturus Engineering). DNase treatment was not performed on  
226 the kit column, as described in the kit protocol, but RNA was treated with Turbo DNase  
227 after the extraction procedure (Applied Biosystems, Foster City, CA, USA), according  
228 with the manufacturer’s instructions. RNA quality and quantity were checked using a  
229 NanoDrop 1000 spectrophotometer (Thermo Scientific, Wilmington, DE, USA). A  
230 One-Step RT-PCR kit (Qiagen, Valencia, CA, USA) was used. Reactions were carried  
231 out in a final volume of 20 µl, as previously described by Balestrini et al. (2007).  
232 Samples were incubated at 50°C for 30 min, then at 95°C for 15 min. Amplification  
233 reactions were run for 40 cycles: 94°C for 45 s, 58°C for 45 s and 72°C for 45 s. All  
234 RT-PCR experiments were performed on at least two biological and two technical  
235 replicates. RNA samples were checked for DNA contamination through RT-PCR  
236 analyses conducted with the *VvEFL-α* specific primers. PCR products were separated on  
237 a 1.9% agarose gel. Target genes and relative primer pairs are described in Table S1.  
238 Semi-quantitative RT-PCR experiments were carried out in a final volume of 21 µl  
239 following the same protocol. Amplification reactions with specific primers for the  
240 selected genes (Table S1) and control gene (*VvEFL-α*) were run for different cycles (35,  
241 37, 40) to determine the exponential amplification phase, as previously reported by  
242 Guether et al. (2009). For each step of semi-quantitative RT-PCR, 7 µl of cDNA were  
243 loaded on a 1.9% agarose gel.

244

245

246 Quantitative expression analysis on whole petioles and leaf ABA concentration

247

248 Expression changes of target transcripts were quantified on whole petiole samples by  
249 quantitative real-time PCR (RT-qPCR). Two leaves per plant were collected at the same  
250 time points of PLC determination. Petioles from each treatment were pooled,  
251 immediately frozen in liquid nitrogen and stored at  $-80^{\circ}\text{C}$ . Total RNA was extracted in  
252 triplicate from the pooled samples following the protocol by Carra et al. (2007). RNA  
253 integrity and quantity were checked using a 2100 Bioanalyser (Agilent, Santa Clara,  
254 CA, USA). RNA samples were treated with DNase I, RNase-free (Fermentas:  $50\text{ U }\mu\text{l}^{-1}$ ),  
255 and first-strand cDNA was synthesised starting from  $10\text{ }\mu\text{g}$  of total RNA by using the  
256 High Capacity cDNA Reverse Transcription kit (Applied Biosystems) following the  
257 manufacturers' instructions.

258 Reactions were carried out in a StepOnePlus<sup>TM</sup> RT-qPCR System (Applied Biosystems)  
259 and the SYBR Green method (Power SYBR<sup>®</sup> Green PCR Master Mix, Applied  
260 Biosystems) was used for quantifying amplification results (Perrone et al. 2012a). Three  
261 technical replicates were run for each sample. Thermal cycling conditions were as  
262 follows: an initial denaturation phase at  $95^{\circ}\text{C}$  for 10 min, followed by 40 cycles at  $95^{\circ}\text{C}$   
263 for 15 s and  $60^{\circ}\text{C}$  for 1 min (only for aquaporin primers a step at  $56^{\circ}\text{C}$  for 15 s was  
264 added to the cycling stage). Specific annealing of primers was checked on dissociation  
265 kinetics performed at the end of each RT-qPCR run. Expression of target transcripts  
266 was quantified after normalisation to the geometric mean of the endogenous control  
267 genes, *Ubiquitin* (*VvUBI*) and *Actin* (*VvACT1*). Gene expression data were calculated as  
268 expression ratios (relative quantity, RQ) to IRR controls. Gene-specific primers are  
269 listed in Table S1. Significant differences between treated and control samples were  
270 investigated by applying a one-way ANOVA test ( $P < 0.05$ ), using the SPSS statistical  
271 software package (SPSS, v.20).

272 Leaf blades for ABA analysis were also immediately frozen at  $-80^{\circ}\text{C}$ , and ABA  
273 concentration was quantified following the method previously described by Lovisolo et  
274 al. (2008).

275

276

277 **Results**

278

279 Leaf physiological parameters and leaf ABA concentration

280

281 Stem pressurisation obtained by application of a pressure collar induces xylem  
282 embolism formation without imposing long-lasting stress on the organs located distally  
283 to the collar. We compared the physiological responses (leaf gas exchange, petiole  
284 xylem embolism, and petiole ABA concentration) induced by application of either the  
285 pressure collar or water stress, and by the following depressurisation or rehydration.

286 As expected, application of the pressure collar effectively induced xylem embolism.  
287 percentage loss of hydraulic conductivity (PLC) was about 10% in IRR petioles. WS  
288 treatment induced an increase in PLC to about 80%, and application of the PC also  
289 induced an increase in PLC to about 60%. Embolism recovery proceeded much faster in  
290 RPC than in RWS petioles: upon irrigation of WS plants, PLC only decreased to 54%  
291 after 27 h from the re-watering treatment, while stem depressurisation (RPC) allowed  
292 almost full recovery from embolism within 3 h (10% PLC) (Fig. 1).

293 Application of the PC also induced water stress in the leaves, as shown by  
294 measurements of leaf water potential ( $\Psi_{\text{leaf}}$ ) and stomatal conductance ( $g_s$ ), albeit at a  
295 lower level than the application of WS. In irrigated (IRR) petioles,  $\Psi_{\text{leaf}}$  remained  
296 relatively constant between  $-0.3$  and  $-0.4$  MPa.  $\Psi_{\text{leaf}}$  decreased to about  $-1.4$  MPa upon  
297 WS, and to about  $-1.2$  MPa upon PC application (Fig. 2a). In IRR plants  $g_s$  averaged  
298  $0.14 \text{ mol m}^{-2} \text{ s}^{-1}$  with an expected slight decrease in the afternoon. Leaf  $g_s$  was lower in  
299 WS plants (less than  $0.03 \text{ mol m}^{-2} \text{ s}^{-1}$ ) and in PC plants  $0.06 \text{ mol m}^{-2} \text{ s}^{-1}$  (Fig. 2b). Leaf  
300 transpiration rate (E) reflected the observed changes in  $g_s$  (Fig. 2c).

301 The behaviour of plants subjected to WS versus PC treatment was, however, quite  
302 different when a recovery was induced by rehydration in the case of WS (RWS), and by

303 depressurisation in the case of PC (RPC). In RWS petioles,  $\Psi_{\text{leaf}}$  recovered very slowly,  
304 reaching -0.5 MPa at 19:00 h the following day, while recovery upon depressurisation  
305 was fast and complete, reaching -0.5 MPa at 19:00 h the following day, while recovery  
306 upon depressurisation was fast and complete, reaching -0.5 MPa within 3 h (Fig. 2a).  
307 Also,  $g_s$  and E recovery were slow in RWS plants, reaching about 50% of that of the  
308 IRR controls at 19:00 h the following day, while, in RPC plants,  $g_s$  quickly (within 3 h)  
309 recovered (Fig. 2b,c).

310 Since the maintenance of responses to water stress after rehydration in grapevine is  
311 dependent on the persistence of stress-induced endogenous ABA, we reasoned that the  
312 physiological differences observed between WS-RWS and PC-RPC plants could be due  
313 to different intensities of an ABA signal. The ABA concentration in leaves of irrigated  
314 plants did not differ from that measured in PC and RPC leaf samples, while in WS leaf  
315 ABA was significantly higher, with values around 13 000 pmol  $g^{-1}$  DW. At the end of  
316 recovery from water stress (RWS), ABA levels dropped to values comparable with  
317 those of the IRR controls (Fig. 3).

318

319 Laser microdissection and analysis of gene expression in vessel-associated cells and  
320 whole petioles

321

322 The LMD protocol preserved petiole vascular tissues fairly well, which allowed  
323 identification of specific cell types, in particular VACs (present among xylem vessels)  
324 and phloem (Fig. 4a,b). For each treatment, about 270–300 vascular cell groups were  
325 obtained. RNA final concentrations ranged between 10 and 30 ng  $\mu l^{-1}$ , depending on  
326 the sample type and on the number of collected vascular cell groups. RNA samples  
327 from the LMD-isolated tissue were then used to study the expression of genes  
328 putatively involved in xylem embolism formation and repair. More specifically, all



329 target transcripts were first analysed in VACs by carrying out one-step RT-PCR  
330 experiments. In RT-plus reactions the presence of an amplified fragment of the expected  
331 size (100 bp) was observed in all cell types tested, using specific primers for the  
332 endogenous control gene *VvEFI- $\alpha$* , while the absence of an amplified product in RT-  
333 minus reactions excluded genomic DNA contamination (Fig. S1). Since for the majority  
334 of the genes an expression signal was observed in several of the considered treatments  
335 (data not shown), we further investigated transcript expression by semi-quantitative  
336 PCR analysis after 35, 37 and 40 amplification cycles (Fig. 4). After 40 cycles, the  
337 amplification had reached its plateau in all samples, whereas after 35 and 37 cycles it  
338 was still in the exponential phase, thus allowing a semi-quantitative comparison of  
339 transcript abundance. As shown in Fig. 4c, transcript abundance of the control gene  
340 *VvEFI- $\alpha$*  was comparable in all samples. We analysed the expression of 12 genes  
341 related to drought and ABA responses to sugar metabolism and to water transport,  
342 which are regulated in grapevine petioles upon water stress and rehydration (Perrone et  
343 al. 2012b). More specifically, we considered: three genes involved in sugar  
344 metabolism—a plastidic glucose-6P transporter (*VvGPT1*), a sucrose transporter  
345 (*VvSUC27*), and a plastidic  $\beta$ -amylase (*VvBAM3*); two genes encoding proteins  
346 belonging to the LEA (Late Embryogenesis Abundant) family (*VvDHN1a* and  
347 *VvLEA14*); three genes encoding components of signal transduction (*VvNAC72*,  
348 *VvSnRK2.1*, and *VvCAL*) and activated by drought and ABA in several systems; and  
349 four genes encoding PIP-type aquaporins—namely *VvPIP1;1*, *VvPIP1;2*, *VvPIP2;1*  
350 (Vandeleur et al. 2009) and *VvPIP2;4N* (Perrone et al. 2012a). Expression analyses  
351 performed on micro-dissected VACs showed that *VvGPT1* was activated by PC and  
352 RPC treatments; *VvSUC27* expression was low in all treatments, while *VvBAM3* was  
353 activated in WS- and PC-treated cells (Fig. 4d,f). Results on genes potentially tied to  
354 signal transduction mechanisms showed that *VvSnRK2.1* was activated in WS petioles,

355 while *VvNAC72*, besides in WS cells, was also activated in PC and RPC samples (Fig.  
356 4g,h); *VvCAL* transcripts were only detected in WS and RWS cells (Fig. 4k). Among  
357 aquaporin genes, *VvPIP1;1* was one of the most highly expressed in embolism-inducing  
358 treatments (WS and PC), but it was also activated in RWS and RPC cells (Fig. 4i).  
359 *VvPIP1;2* expression was undetectable in all treatments (data not shown). *VvPIP2;1*  
360 was more expressed in PC and RPC treatments than in the other treatments (Fig. 4j);  
361 however, *VvPIP2;4N* transcripts were only observed in WS and mostly in RWS cells  
362 (Fig. 4l). Considering the members of the LEA family, which are typically involved in  
363 plant stress response, *VvDHN1a* was exclusively expressed in WS and PC cell samples,  
364 whereas *VvLEA14* was mainly activated in PC and in RPC cells and to a lesser extent in  
365 WS cells (Fig. 4m,n).

366 To verify the specificity of gene expression in VACs, quantitative real-time PCR (RT-  
367 qPCR) experiments were performed on the same target genes working on whole petiole  
368 samples. *VvGPT1* and *VvSUC27* expression followed the same patterns observed in  
369 VACs (Fig. 5a,b). *VvBAM3* was significantly activated upon WS treatment (as in  
370 VACs), but it was down-regulated in PC and RPC petioles, despite these latter  
371 expression changes were not significant when compared to the IRR control (Fig. 5c).  
372 The two *LEA* genes were both strongly up-regulated upon WS treatment and their  
373 expression was still very high in RWS samples (Fig. 5d,e). Moreover, *VvLEA14* was  
374 significantly over-expressed in PC petioles, mirroring the pattern observed in VACs  
375 (Fig. 5d). No significant changes were observed for *VvDHN1a* transcripts in PC  
376 samples compared to the IRR control (Fig. 5e), while the same gene was activated in  
377 VACs upon this treatment.

378 In whole petiole, the expression of genes encoding components of signal transduction  
379 followed patterns similar to those observed in VACs: both *VvNAC72* and *VvSnRK2;1*  
380 levels increased in WS and RWS treatments (Fig. 5f,g), although the over-expression of

381 *VvSnRK2;1* was significant only in WS samples (Fig. 5g). Interestingly, *VvNAC72* was  
382 also slightly activated in PC and RPC treatments (Fig. 5f), whereas  
383 *VvSnRK2;1* transcripts underwent a significant down-regulation.

384 The same consideration can be made for *VvCAL* transcripts, which were highly  
385 expressed in WS and RWS petioles, following the expression profile observed in VACs,  
386 while they were significantly down-regulated in both PC and RPC samples (Fig. 5h).

387 Among aquaporin genes, *VvPIP1;1* was slightly activated in WS petioles and  
388 significantly down-regulated in RWS, PC and RPC petioles (Fig. 6a), at variance with  
389 the observations made in VACs; *VvPIP1;2* was up-regulated in all treatments compared  
390 to the IRR control (Fig. 6b), whereas in all VAC samples the same gene was not  
391 detected.

392 Finally, while the expression of *VvPIP2;1* followed the same pattern observed in VACs  
393 (it strongly increased in PC and RPC), *VvPIP2;4N* transcriptional levels were  
394 significantly down-regulated in all treatments (Fig. 6c,d).

395

396

397

## 398 **Discussion**

399

400 Induction of xylem embolism in grapevine by water stress and stem pressurisation

401

402 It is well known that water stress (and subsequent rehydration) can induce xylem  
403 embolism formation and recovery. Nevertheless, this environmental condition triggers a  
404 wide array of molecular changes, which can mask those strictly related to embolism  
405 refilling processes. In order to control these masking effects, we employed, parallel to  
406 water stress and rehydration, the technique of stem pressurisation/depressurisation to

407 induce embolism formation and repair with a limited incidence of other stress-induced  
408 processes. Both water stress and stem pressurisation require petiole excision to assess  
409 the degree of embolism, and this was reported to induce artefacts on *Acer rubrum* and  
410 *Fraxinus americana* (Wheeler et al. 2013). However, direct observations of embolism  
411 recovery obtained in the absence of petiole excision (Brodersen et al. 2010, 2013)  
412 suggest that refilling in grapevine is not affected by such artefacts (Sperry, 2013).

413 In our experiment, stem pressurisation was obtained by applying a pressure collar to  
414 grape stems. Other authors have already used artificial tools to induce xylem cavitation  
415 in woody plants (e.g., Salleo et al. 1996; Mayr et al. 2006; Secchi and Zwieniecki  
416 2011). These systems are particularly suited to increasing pressure gradients at air-water  
417 interfaces into the plant organs, thus inducing embolism formation. The method we set  
418 up avoids both air injection bores and wounding to create the air inlet. After about five  
419 hours of PC treatment, PLC increased from 10% to 55% in petioles; following  
420 depressurisation, PLC fully recovered within 3 hours.

421 The PC treatment was not devoid of effects on water potential and leaf gas exchange,  
422 which decreased after pressurisation and recovered upon depressurisation. Nevertheless,  
423 the time courses of PLC, water potential, and leaf gas exchange upon RPC and RWS  
424 were clearly different, since RPC recovery kinetics were more rapid. Depressurised  
425 twigs of laurel, previously submitted to a pressure collar treatment, showed faster and  
426 larger xylem refilling than upon native embolism repair (Salleo et al. 1996). A slow  
427 recovery of hydraulic conductance and transpiration after rehydration of drought-  
428 exposed plants has been well documented in grapevine and linked to the persistence of  
429 high ABA concentration after rehydration (Lovisolo et al. 2008; Flexas et al. 2009;  
430 Zufferey et al. 2011; Perrone et al. 2012b). ‘Grenache’ is a drought-avoiding isohydric  
431 grape genotype, particularly suited to study drought responses, since it is able to tolerate  
432 long-term water stress conditions (Schultz 2003; Soar et al. 2004; Vandeleur et al. 2009)

433 through ABA-mediated control of stomatal closure (Lovisolo et al. 2008, 2010). In this  
434 experiment, recovery in RPC plants was indeed associated with low leaf ABA  
435 concentration.

436 Differences in leaf ABA concentration, and in the kinetics and intensity of leaf water  
437 potential and gas exchange changes induced by the two types of treatment, likely reflect  
438 diverse mechanisms of induction of xylem embolism. In the case of drought-induced  
439 water stress, water status is negatively affected, and ABA concentration increases in the  
440 leaves, inducing stomatal closure: increased PLC is thought to depend on the increased  
441 xylem tension that develops as an effect of water potential changes. In the case of stem  
442 pressurisation, no water loss takes place, and xylem embolism is likely the primary  
443 effect, later followed by limitations of leaf water potential due to reduced xylem  
444 hydraulic conductivity, and by stomatal closure. In this case, a reversible loss of leaf  
445 hydraulic conductivity could be a means of amplifying the signal of evaporative  
446 demand to the stomata in order to trigger the stomatal response, as suggested by  
447 Brodribb and Holbrook (2004) and shown in grapevine by Zufferey et al. (2011).

448

449 Expression changes of genes putatively involved in embolism recovery

450

451 Embolism recovery is an active process, which requires energy and metabolic activity.  
452 It takes place upon negative tensions in the xylem, and several mechanistic models have  
453 been proposed to explain it. All these models converge in considering the pivotal role of  
454 solutes, solute transporters, and water transport facilitators (aquaporins) in VACs.  
455 Recently, two studies based on transcriptomic analysis of tissues undergoing embolism  
456 recovery have reported some genes linked to these processes, which undergo significant  
457 expression changes (Secchi et al. 2011; Perrone et al. 2012b). Nevertheless, these  
458 studies have focused on whole tissues, where molecular processes localised in VACs

459 may not be detectable. To deepen the role of these genes, we have analysed the  
460 expression of some of these transcripts in VACs isolated by LMD.

461 The importance of regulation of carbohydrate metabolism and transport in VACs during  
462 the embolism recovery process has already been supported by physiological analyses  
463 (Salleo et al. 1996; Nardini et al. 2011; Secchi et al. 2013) and by measurements of gene  
464 expression changes (Secchi et al. 2011; Perrone et al. 2012b). *VvBAM3* encodes a beta-  
465 amylase up-regulated by water stress (Perrone et al. 2012b) as its *Arabidopsis*  
466 orthologue (Fulton et al. 2008). *VvGPT1* is annotated as a plastidic glucose-6P  
467 symporter and is up-regulated upon embolism recovery (Perrone et al. 2012b). Its  
468 closest *Arabidopsis* homologue, the Glc6P/phosphate translocator1 (*AtGPT1*), is  
469 localised in vascular bundle sheath cells (Niewiadomski et al. 2005), where it  
470 contributes to glucose-6-phosphate transport into plastids (Kunz et al. 2010). In grape  
471 petioles, *VvGPT1* could operate in the reverse direction, providing a supply of GLU-6P  
472 into the cytosol of VACs. *VvGPT1* and *VvBAM3* genes were both activated in VACs  
473 upon the embolism-inducing treatments applied (WS and PC). This data is in agreement  
474 with a picture of activated starch hydrolysis and GLU-6P export from plastids, which  
475 provides soluble sugars required to support the embolism recovery process. *VvSUC27* is  
476 an H<sup>+</sup>-dependent sucrose transporter, whose expression is associated with sink organs in  
477 grape (Davies et al. 1999). In whole grape petioles, *VvSUC27* is down-regulated by all  
478 treatments inducing embolism formation, and it has previously been observed to be also  
479 down-regulated due to water stress (Perrone et al. 2012b). This suggests that, upon  
480 xylem embolism, the main provision of sugars to VACs derives from starch breakdown  
481 and not from phloem unloading. *VvSUC27* expression was almost absent in VACs,  
482 where phloem cells are not present. However, the regulatory changes involving these  
483 genes were not limited to VACs. Indeed, they were also detected in whole petioles,

484 suggesting that most of the petiole cells collaborate each other to the mobilisation of  
485 soluble sugars that drives embolism recovery.

486 The picture was quite different in the case of aquaporins, which are thought to facilitate  
487 water supply to the xylem, thus determining a successful refilling process (Kaldenhoff  
488 et al. 2008). This hypothesis requires that the activation of these channels takes place in  
489 the cells surrounding xylem vessels. Among the tested *PIP1* and *PIP2* genes, *VvPIP1;1*,  
490 *VvPIP2;1* and *VvPIP2;4N* were expressed in VACs of either embolising or recovering  
491 petioles, confirming a potential role for these proteins in embolism refilling. However,  
492 in the case of *VvPIP1;1* and *VvPIP2;4N* genes, these expression differences were not  
493 observed in whole petioles, both in this study and in a previous work by Perrone et al.  
494 (2012b), suggesting that their activation was strictly localised in VACs. The role of  
495 aquaporins in embolism refilling has been inferred from expression measurements  
496 performed in different plants, such as olive (Secchi et al. 2007), grapevine (Galmés et  
497 al. 2007), rice (Sakurai-Ishikawa et al. 2011), tobacco (Mahdieh et al. 2008), and poplar  
498 (Secchi et al. 2011). Aquaporins could contribute to embolism refilling only indirectly,  
499 by facilitating axial flow of water to the leaves and thus reducing the xylem tension  
500 gradient. Our expression results, obtained for the first time at the VAC level, strengthen  
501 the hypothesis that these aquaporins play a pivotal role in refilling xylem embolism.

502 On the contrary, *VvPIP2;1* follows a different model. Indeed, the activation of this gene  
503 takes place both in VACs and whole petioles, suggesting that it is probably not directly  
504 linked to either embolism formation or recovery, but it could indirectly contribute to the  
505 process. Finally, *VvPIP1;2* was activated in petioles but not in VACs, and this points to  
506 a dependency on stress but not to a role in embolism refilling.

507

508 Water-stress and pressure collar responses to xylem embolism

509

510 In PC plants, embolism induction and recovery were faster than in WS plants, and they  
511 took place in the absence of an ABA confounding effect. Since ABA strictly controls  
512 gene expression networks in plants and grapevine (Koyama et al. 2009), we thus  
513 checked whether expression of genes induced by water stress and of genes involved in  
514 embolism recovery could be affected by the two different treatments.

515 Two genes belonging to the late embryogenesis abundant (LEA) protein family,  
516 encoding a LEA14 (*VvLEA14*) and a dehydrin (*VvDHN1a*), were tested. In *Arabidopsis*,  
517 the *VvDHN1a* orthologue (AT1G07470) is activated by salt and cold stress, and by  
518 ABA (Hundertmark et al. 2008). In grapevine, *VvDHN1a* expression is induced by  
519 water stress (Cramer et al. 2007) and ABA (Koyama et al. 2009; Yang et al. 2012). Our  
520 results show that both genes are activated upon WS in VACs and whole petiole  
521 samples, as previously observed in cv. Cabernet Sauvignon by Cramer et al. (2007).  
522 Nevertheless, in VACs these genes were also up-regulated upon PC treatment.

523 We further measured the expression of three stress-responsive genes involved in signal  
524 transduction (*VvCAL*, *VvSnRK2;1*, *VvNAC72*). In detail, *VvCAL* is the grape orthologue  
525 of the *AtCLM24* (AT5G37770) gene, which encodes a Ca<sup>2+</sup> binding protein in response  
526 to ABA stimulus, day length and salt stress (Delk et al. 2005). *VvSnRK2;1* encodes a  
527 protein kinase involved in ABA signal transduction, strongly up-regulated in grape  
528 leaves treated with exogenous ABA (Boneh et al. 2012). *VvNAC72* is the grape  
529 orthologue of *AtNAC72* (AT4G27410), whose expression is strictly controlled by ABA  
530 (Fujita et al. 2004); in grape petioles this gene is activated upon water stress (Perrone et  
531 al. 2012b). Our results indicate that *VvCAL* is only activated in WS and RWS VACs,  
532 and in WS whole petioles; *VvSnRK2;1* transcripts are more abundant upon WS both in  
533 VACs and whole petioles, although a slight up-regulation of this gene could be  
534 observed in VACs upon PC, RPC and RWS treatments. On the contrary, *VvNAC72* is  
535 more expressed in PC and RPC VACs.



536 Such differences between the two treatments were also observed for genes putatively  
537 related to embolism recovery. Expression of *VvPIP2;4N*, and, to a lesser extent of  
538 *VvBAM3*, increased upon water stress. *VvPIP2;4N* is a root-specific grape aquaporin  
539 (Perrone et al. 2012a) and the localisation of its expression in VACs, depending on  
540 water stress, could explain the fact that this transcript is not detected in whole petioles.  
541 In olive twigs it has been shown that *OePIP2;1* aquaporin expression is activated when  
542 shoot hydraulic conductance recovers (Secchi et al. 2007), and generally there is an up-  
543 regulation of aquaporin genes when rehydration also occurs in grapevine leaves  
544 (Galmés et al. 2007) or petioles (Perrone et al. 2012b). In addition, a coupling of  
545 aquaporin activation with an increment in leaf transpiration has also been reported in  
546 rice roots, where transpiration demand triggers the up-regulation of PIPs localised both  
547 at the proximal end of the endodermis and on the cell surface around xylem (Sakurai-  
548 Ishikawa et al. 2011), and in drought-exposed/rehydrated tobacco roots (Mahdieh et al.  
549 2008). An obvious candidate for gene activation exclusively under drought stress is a  
550 surge in ABA concentration, and correspondingly we found no ABA increase in PC and  
551 RPC-treated leaves. We have previously shown (Lovisololo et al. 2008; Perrone et al.  
552 2012b) that, upon rehydration from water stress, grapevine leaves accumulate ABA at  
553 levels even higher than during the stress itself, and this could be instrumental to  
554 embolism recovery if contemporaneously VAC-specific aquaporins are activated as is  
555 the case of *VvPIP2;4N*.

556 Other genes (*VvGPT1* and *VvPIP2;1*) are present only upon pressure collar  
557 pressurisation and depressurisation. These treatments thus trigger embolism-induced  
558 signals that are not induced in water-stressed plants, although embolism is also present  
559 in the latter. An explanation for this apparently contradictory result can be found in the  
560 different dynamics of embolism induction and recovery deriving from the two types of  
561 treatment. These dynamics are much faster in PC and RPC treatments. This means that,

562 during PC and RPC treatments, a fast induction of embolism could elicit signals that are  
563 not present when a slow induction of embolism occurs, such as the case of water stress  
564 treatment. Secchi and Zwieniecki (2010), also using an artificial device to induce  
565 formation of xylem embolism in poplar, proposed several possible signals evoked  
566 during fast embolism induction, such as the accumulation of soluble sugars in the xylem  
567 or oxidative stress. However, in natural (and agricultural) conditions, xylem embolism  
568 almost invariably arises because of drought. The experimental use of devices, such as  
569 the pressure collar, which is applied to obtain embolism in the absence of water stress,  
570 could not be representative of this condition, since this condition seems to activate  
571 genes that are not expressed by water stress and following recovery.

572

573

#### 574 **Acknowledgements**

575 This work was financially supported by AGER foundation, grant n° 2010-2105. The  
576 authors wish to acknowledge Giorgio Gambino and Fabiano Sillo for suggestions and  
577 technical help during molecular analyses. Vivai Cooperativi Rauscedo (Italy) are also  
578 gratefully acknowledged.

579

580 **References**

581

582 Angeles G, Bond B, Boyer JS, Brodribb T, Brooks JR, Burns MJ, Cavender-Bares J,  
583 Clearwater M, Cochard H, Comstock J et al (2004) The cohesion-tension theory. *New*  
584 *Phytol* 163:451–452

585 Balestrini R, Gomez-Ariza J, Lanfranco L, Bonfante P (2007) Laser microdissection  
586 reveals that transcripts for five plant and one fungal phosphate transporter genes are  
587 contemporaneously present in arbusculated cells. *Mol Plant Microbe Interact* 20:1055–  
588 1062

589 Balestrini R, Gomez-Ariza J, Klink VP, Bonfante P (2009) Application of laser  
590 microdissection to plant pathogenic and symbiotic interactions. *J Plant Interact* 4:81–92.

591 Boneh U, Biton I, Schwartz A, Ben-Ari G (2012) Characterization of the ABA signal  
592 transduction pathway in *Vitis vinifera*. *Plant Sci* 187:89–96

593 Brodersen CR, McElrone AJ, Choat B, Matthews MA, Shackel KA (2010) The  
594 dynamics of embolism repair in xylem: *in vivo* visualizations using high-resolution  
595 computed tomography. *Plant Physiol* 154:1088–1095

596 Brodersen CR, McElrone AJ, Choat B, Lee EF, Shackel KA, Matthews MA (2013) *In*  
597 *vivo* visualizations of drought-induced embolism spread in *Vitis vinifera*. *Plant Physiol*  
598 161:1820–1829

599 Brodribb TJ, Holbrook NM (2004) Diurnal depression of leaf hydraulic conductance in  
600 a tropical tree species. *Plant Cell Environ* 27:820–827

601 Carra A, Gambino G, Schubert A (2007) A cetyltrimethylammonium bromide-based  
602 method to extract low-molecular-weight RNA from polysaccharide-rich plant tissues.  
603 *Anal Biochem* 360:318–320

604 Chandran D, Inada N, Hather G, Kleindt CK, Wildermuth MC (2010) Laser  
605 microdissection of *Arabidopsis* cells at the powdery mildew infection site reveals site-  
606 specific processes and regulators. *Proc Natl Acad Sci USA* 107:460–465

607 Choat B, Gambetta GA, Shackel K, Matthews MA (2009) Vascular function in grape  
608 berries across development and its relevance to apparent hydraulic isolation. *Plant*  
609 *Physiol* 151:1677–1687

610 Clearwater M, Goldstein G (2005) Embolism repair and long distance water transport.  
611 In: Holbrook NM, Zwieniecki MA (eds) *Vascular transport in plants*. Elsevier  
612 Academic Press, Burlington, MA, pp 375–399

613 Cramer GR, Ergül A, Grimplet J, Tillet RL, Tattersall EAR, Bohlman MC, Vincent D,  
614 Sonderegger J, Evans J, Osborne C, Quilici D, Schlauch KA, Schooley DA, Cushman  
615 JC (2007) Water and salinity stress in grapevines: early and late changes in transcript  
616 and metabolite profiles. *Funct Integr Genomics* 7:111–134

617 Davies C, Wolf T, Robinson SP (1999) Three putative sucrose transporters are  
618 differentially expressed in grapevine tissues. *Plant Sci* 147:93–100

619 Davis SD, Ewers FW, Sperry JS, Portwood KA, Crocker MC, Adams GC (2002) Shoot  
620 dieback during prolonged drought in *Ceanothus* (*Rhamnaceae*) chaparral of California:  
621 a possible case of hydraulic failure. *Am J Bot* 89:820–828

622 Delk NA, Johnson KA, Chowdhury NI, Braam J (2005) CML24, regulated in  
623 expression by diverse stimuli, encodes a potential Ca<sup>2+</sup> sensor that functions in  
624 responses to abscisic acid, daylength, and ion stress. *Plant Physiol* 139:240–253

625 Flexas J, Barón M, Bota J, Ducruet J-M, Gallé A, Galmés J, Jiménez M, Pou A, Ribas-  
626 Carbó M, Sajnani C (2009) Photosynthesis limitations during water stress acclimation  
627 and recovery in the drought-adapted *Vitis* hybrid Richter-110 (*V. berlandieri* x *V.*  
628 *rupestris*). *J Exp Bot* 60:2361–2377

629 Fujita M, Fujita Y, Maruyama K, Seki M, Hiratsu K, Ohme-Takagi M, Phan Tran L-S,  
630 Yamaguchi-Shinozaki K, Shinozaki K (2004) A dehydration-induced NAC protein,  
631 RD26, is involved in a novel ABA-dependent stress-signalling pathway. *Plant J*  
632 39:863–876

633 Fulton DC, Stettler M, Mettler T, Vaughan KC, Li J, Francisco P, Gil M, Reinhold H,  
634 Eicke S, Messerli G et al (2008) B-AMYLASE4, a noncatalytic protein required for  
635 starch breakdown, acts upstream of three active  $\beta$ -amylases in *Arabidopsis* chloroplasts.  
636 *Plant Cell* 20:1040–1058

637 Galmés J, Pou A, Alsina MM, Tomàs M, Medrano H, Flexas J (2007) Aquaporin  
638 expression in response to different water stress intensities and recovery in Richter-110  
639 (*Vitis* spp.): relationship with ecophysiological status. *Planta* 226:671–681

640 Giovannetti M, Balestrini R, Volpe V, Guether M, Straub D, Costa A, Ludewig U,  
641 Bonfante P (2012) Two putative-aquaporin genes are differentially expressed during  
642 arbuscular mycorrhizal symbiosis in *Lotus japonicus*. *BMC Plant Biol* 12:186.  
643 doi:10.1186/1471-2229-12-186

644 Gomez SK, Harrison MJ (2009) Laser microdissection and its application to analyze  
645 gene expression in arbuscular mycorrhizal symbiosis. *Pest Manag Sci* 65:504–511.

646 Guether M, Neuhäuser B, Balestrini R, Dynowski M, Ludewig U, Bonfante P (2009) A  
647 mycorrhizal-specific ammonium transporter from *Lotus japonicus* acquires nitrogen  
648 released by arbuscular mycorrhizal fungi. *Plant Physiol* 150:73–83

649 Holbrook NM, Zwieniecki MA (1999) Xylem refilling under tension. Do we need a  
650 miracle? *Plant Physiol* 120:7–10

651 Holbrook NM, Ahrens ET, Burns MJ, Zwieniecki MA (2001) *In vivo* observation of  
652 cavitation and embolism repair using magnetic resonance imaging. *Plant Physiol*  
653 126:27–31

654 Hundertmark M, Hinch KD (2008) LEA (Late Embryogenesis Abundant) proteins and  
655 their encoding genes in *Arabidopsis thaliana*. *BMC Genomics* 9:1–18

656 Just J, Sauter JJ (1991) Changes in hydraulic conductivity upon freezing of the xylem of  
657 *Populus x canadensis* Moench ‘robusta’. *Trees* 5:117–121

658 Kaldenhoff R, Ribas-Carbo M, Flexas J, Lovisolo C, Heckwolf M, Uehlein N (2008)  
659 Aquaporins and plant water balance. *Plant Cell Environ* 31:658–666

660 Kerk NM, Ceserani T, Tausta SL, Sussex IM, Nelson TM (2003) Laser capture  
661 microdissection of cells from plant tissues. *Plant Physiol* 132:27–35

662 Koyama K, Sadamatsu K, Goto-Yamamoto N (2009) Abscisic acid stimulated ripening  
663 and gene expression in berry skins of the Cabernet Sauvignon grape. *Funct Integr*  
664 *Genomics* 10:367–381

665 Kunz HH, Häusler RE, Fettke J, Herbst K, Niewiadomski P, Gierth M, Bell K, Steup  
666 M, Flügge UI, Schneider A (2010) The role of plastidial glucose-6-phosphate/phosphate  
667 translocators in vegetative tissues of *Arabidopsis thaliana* mutants impaired in starch  
668 biosynthesis. *Plant Biol* 12(Suppl.1):115–128

669 Lovisolo C, Schubert A (1998) Effects of water stress on vessel size and xylem  
670 hydraulic conductivity in *Vitis vinifera* L. *J Exp Bot* 49:693–700

671 Lovisolo C, Schubert A (2006) Mercury hinders recovery of shoot hydraulic  
672 conductivity during grapevine rehydration: evidence from a whole-plant approach. *New*  
673 *Phytol* 172:69–478

674 Lovisolo C, Perrone I, Hartung W, Schubert A (2008) An abscisic acid-related reduced  
675 transpiration promotes gradual embolism repair when grapevines are rehydrated after  
676 drought. *New Phytol* 180:642–651

677 Lovisolo C, Perrone I, Carra A, Ferrandino A, Flexas J, Medrano H, Schubert A (2010)  
678 Drought-induced changes in development and function of grapevine (*Vitis* spp.) organs

679 and in their hydraulic and non-hydraulic interactions at the whole-plant level: a  
680 physiological and molecular update. *Funct Plant Biol* 37:98–116

681 Mahdiah M, Mostajeran A, Horie T, Katsuhara M (2008) Drought stress alters water  
682 relations and expression of PIP-type aquaporin genes in *Nicotiana tabacum* plants. *Plant*  
683 *Cell Physiol* 49:801–813

684 Mayr S, Rothart B, Wolfschwenger M (2006) Temporal and spatial pattern of embolism  
685 induced by pressure collar techniques in twigs of *Picea abies*. *J Exp Bot* 57:3157–3163

686 Nardini A, Salleo S, Lo Gullo MA, Pitt F (2000) Different responses to drought and  
687 freeze stress of *Quercus ilex* L. growing along a latitudinal gradient. *Plant Ecol*  
688 148:139–147

689 Nardini A, Lo Gullo MA, Salleo S (2011) Refilling embolised xylem conduits: Is it a  
690 matter of phloem unloading? *Plant Sci* 180:604–611

691 Niewiadomski P, Knappe S, Geimer S, Fischer K, Schulz B, Unte US, Rosso MG, Ache  
692 P, Flügge UI, Schneider A (2005) The Arabidopsis plastidic glucose 6-  
693 phosphate/phosphate translocator GPT1 is essential for pollen maturation and embryo  
694 sac development. *Plant Cell* 17:760–775

695 Perrone I, Gambino G, Chitarra W, Vitali M, Pagliarani C, Riccomagno N, Balestrini R,  
696 Kaldenhoff R, Uehlein N, Gribaudo I et al (2012a) The grapevine root-specific  
697 aquaporin *VvPIP2;4N* controls root hydraulic conductance and leaf gas exchange upon  
698 irrigation but not under water stress. *Plant Physiol* 160:965–977

699 Perrone I, Pagliarani C, Lovisolo C, Chitarra W, Roman F, Schubert A (2012b)  
700 Recovery from water stress affects grape leaf petiole transcriptome. *Planta* 235:1383–  
701 1396

702 Reid KE, Olsson N, Schlosser J, Peng F, Lund ST (2006) An optimized grapevine RNA  
703 isolation procedure and statistical determination of reference genes for real-time RT-  
704 PCR during berry development. *BMC Plant Biol* 6:27. doi:10.1186/1471-2229-6-27

705 Sakr S, Alves G, Morillon RL, Maurel K, Decourteix M, Guilliot A, Fleurat-Lessard P,  
706 Julien JL, Chrispeels MJ (2003) Plasma membrane aquaporins are involved in winter  
707 embolism recovery in walnut tree. *Plant Physiol* 133:630–641

708 Sakurai-Ishikawa J, Murai-Hatano M, Hayashi H, Ahamed A, Fukushi K, Matsumoto  
709 T, Kitagawa Y (2011) Transpiration from shoots triggers diurnal changes in root  
710 aquaporin expression. *Plant Cell Environ* 34:1150–1163

711 Salleo S, Lo Gullo MA, De Paoli D, Zippo M (1996) Xylem recovery from cavitation-  
712 induced embolism in young plants of *Laurus nobilis*: a possible mechanism. *New*  
713 *Phytol* 132:47–56

714 Salleo S, Lo Gullo MA, Trifilo P, Nardini A (2004) New evidence for a role of vessel-  
715 associated cells and phloem in the rapid xylem refilling of cavitated stems of *Laurus*  
716 *nobilis* L. *Plant Cell Environ* 27:1065–1076

717 Salleo S, Trifilò P, Esposito S, Nardini A, Lo Gullo MA (2009) Starch-to-sugar  
718 conversion in wood parenchyma of field-growing *Laurus nobilis* plants: a component of  
719 the signal pathway for embolism repair? *Funct Plant Biol* 36:815–825

720 Schultz HR, Matthews MA (1988) Resistance to water transport in shoots of *Vitis*  
721 *vinifera* L.: relation to growth at low water potential. *Plant Physiol* 88:718–724

722 Schultz HR (2003) Differences in hydraulic architecture account for near-isohydric and  
723 anisohydric behaviour of two field-grown *Vitis vinifera* L. cultivars during drought.  
724 *Plant Cell Environ* 26:1393–1405

725 Secchi F, Lovisolo C, Schubert A (2007) Expression of *OePIP2.1* aquaporin gene and  
726 water relations of *Olea europaea* L. twigs during drought stress and recovery. *Ann Appl*  
727 *Biol* 150:163–167

728 Secchi F, Zwieniecki MA (2010) Patterns of *PIP* gene expression in *Populus*  
729 *trichocarpa* during recovery from xylem embolism suggest a major role for the PIP1



730 aquaporin subfamily as moderators of refilling process. *Plant Cell Environ* 33:1285–  
731 1297.

732 Secchi F, Gilbert ME, Zwieniecki MA (2011) Transcriptome response to embolism in  
733 stems of *P. trichocarpa*. *Plant Physiol* 157:1419–1429

734 Secchi F, Zwieniecki MA (2011) Sensing embolism in xylem vessels: the role of  
735 sucrose as a trigger for refilling. *Plant Cell Environ* 34:514–524

736 Secchi F, Zwieniecki MA (2012) Analysis of xylem sap from functional  
737 (nonembolised) and nonfunctional (embolised) vessels of *Populus nigra*: chemistry of  
738 refilling. *Plant Physiol* 160:955–964

739 Secchi F, Perrone I, Chitarra W, Zwieniecka AK, Lovisolo C, Zwieniecki MA (2013)  
740 The dynamics of embolism refilling in abscisic acid (ABA)-deficient tomato plants. *Int*  
741 *J Mol Sci* 14:359–377

742 Soar CJ, Speirs J, Maffei SM, Loveys BR (2004) Gradients in stomatal conductance,  
743 xylem sap ABA and bulk leaf ABA along canes of *Vitis vinifera* cv. Shiraz: molecular  
744 and physiological studies investigating their source. *Funct Plant Biol* 31:659–669

745 Sperry JS (2013) Cutting-edge research or cutting-edge artefact? An overdue control  
746 experiment complicates the xylem refilling story. *Plant Cell Environ* 36:1916–1918

747 Tramontini S, Vitali M, Centioni L, Schubert A, Lovisolo C (2013) Rootstock control  
748 of scion response to water stress in grapevine. *Environ Exp Bot* 93:20–26

749 Tyree MT, Kolb KJ, Rood SB, Patino S (1994) Vulnerability to drought-induced  
750 cavitation of riparian cottonwoods in Alberta: a possible factor in the decline of the  
751 ecosystem? *Tree Physiol* 14:455–466

752 Tyree MT, Patiño S, Bennink J, Alexander J (1995) Dynamic measurements of root  
753 hydraulic conductance using a high-pressure flowmeter in the laboratory and field. *J*  
754 *Exp Bot* 46:83–94

755 Tyree MT, Salleo S, Nardini A, Lo Gullo MA, Mosca R (1999) Refilling of embolised  
756 vessels in young stems of laurel. Do we need a new paradigm? *Plant Physiol* 120:11–21

757 Tyree MT (2003) Plant hydraulics: the ascent of water. *Nature* 423:923

758 Vandeleur RK, Mayo G, Shelden MC, Gilliam M, Kaiser BN, Tyerman SD (2009)  
759 The role of plasma membrane intrinsic protein aquaporins in water transport through  
760 roots: diurnal and drought stress responses reveal different strategies between isohydric  
761 and anisohydric cultivars of grapevine. *Plant Physiol* 149:445–460

762 Wheeler JK, Huggett BA, Tofte AN, Rockwell FE, Holbrook NM (2013) Cutting xylem  
763 under tension or supersaturated with gas can generate PLC and the appearance of rapid  
764 recovery from embolism. *Plant Cell Environ* 36:1938-1949

765 Yang Y, He M, Zhu Z, Li S, Xu Y, Zhang C, Singer SD, Wang Y (2012) Identification  
766 of the *dehydrin* gene family from grapevine species and analysis of their responsiveness  
767 to various forms of abiotic and biotic stress. *BMC Plant Biol* 12:140.  
768 doi:10.1186/1471-2229-12-140

769 Zufferey V, Cochard H, Ameglio T, Spring JL, Viret O (2011) Diurnal cycles of  
770 embolism formation and repair in petioles of grapevine (*Vitis vinifera* cv. Chasselas). *J*  
771 *Exp Bot* 62:3885–389

772

773

774 **Figure captions**

775

776 **Fig. 1** Percentage loss of hydraulic conductivity (PLC) measured on cv. Grenache  
777 petioles. IRR, irrigated control; WS, water stress; RWS, recovery from water stress; PC,  
778 pressure collar stress; RPC, recovery from pressure collar stress. Lower case letters  
779 denote significant differences ( $P < 0.05$ ) attested by using the Tukey's test, bars are  
780 standard errors of the mean ( $n = 4$ )

781

782 **Fig. 2** Time course of daily changes in leaf water potential ( $\Psi_{\text{leaf}}$ , **a**), stomatal  
783 conductance ( $g_s$ , **b**), and leaf transpiration ( $E$ , **c**), measured on cv. Grenache plants well  
784 watered (IRR), subjected to water stress (WS) and pressure collar (PC) treatments. Gray  
785 arrow displays the time of PC pressurisation and black arrow shows the time of both  
786 WS re-watering and PC depressurisation, as described in Materials and Methods. Bars  
787 are standard errors of the mean ( $n = 4$ ). Boxes containing initials are positioned  
788 according with the sampling time. IRR, irrigated control; WS, water stress; RWS,  
789 recovery from water stress; PC, pressure collar stress; RPC, recovery from pressure  
790 collar stress

791

792 **Fig. 3** ABA concentration ( $\text{pmol g}^{-1} \text{DW}$ ) in leaves of cv. Grenache plants. Lower case  
793 letters denote significant differences ( $P < 0.05$ ) attested by using the Tukey's test; bars  
794 are standard errors of the mean ( $n = 4$ )

795

796

797 **Fig. 4** Microdissection of vessel associated cells around xylem vessels (target section  
798 area is indicated with a black line) before **(a)** and after **(b)** laser cutting. The inset shows  
799 collected cells; red arrows indicate vessel-associated cells. Pictures were taken using an  
800 x40 objective lens; scale bars represent 50  $\mu$ m. Xyl: xylem cells; Phl: phloem cells.

801 **c-j** Semi-quantitative RT-PCR analyses on micro-dissected cells using the elongation  
802 factor gene (*VvEF1- $\alpha$* ) **(c)** as endogenous control. Numbers correspond to RT-PCR  
803 cycles. **k-n** RT-PCR on micro-dissected cells using specific primers for *VvCAL* **(k)**,  
804 *VvPIP2;4N* **(l)**, *VvDHN1a* **(m)** and *VvLEA14* **(n)** genes. The size of amplified sequences  
805 is 100 bp. IRR, irrigated control; WS, water stress; RWS, recovery from water stress;  
806 PC, pressure collar stress; RPC, recovery from pressure collar stress

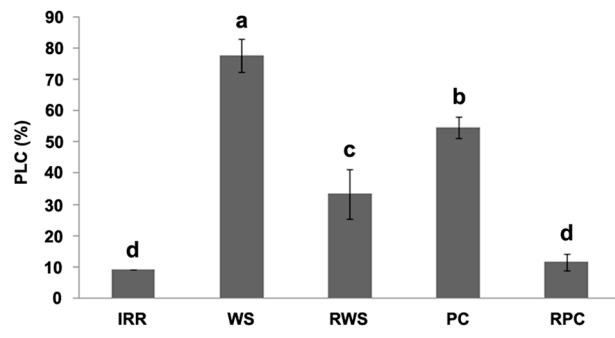
807

808 **Fig. 5** Expression analysis of target genes in whole petioles: **a-h** RT-qPCR analyses on  
809 cv. Grenache petioles for *VvGPT1* **(a)**, *VvSUC27* **(b)**, *VvBAM3* **(c)**, *VvLEA14* **(d)**,  
810 *VvDHN1a* **(e)**, *VvNAC72* **(f)**, *VvSnRK2;1* **(g)** and *VvCAL* **(h)** transcripts. *Ubiquitin*  
811 (*VvUBI*) and *Actin1* (*VvACT1*) were used as endogenous control genes for the  
812 normalisation procedure. IRR, irrigated control; WS, water stress; RWS, recovery from  
813 water stress; PC, pressure collar stress; RPC, recovery from pressure collar stress.  
814 Lower case letters denote significant differences ( $P < 0.05$ ) attested by using the  
815 Tukey's test, bars are standard errors of the mean ( $n = 3$ ).

816

817 **Fig. 6** Expression analysis of target aquaporin genes in whole petioles: **a-d** RT-qPCR  
818 analyses on cv. Grenache petioles for *VvPIP1;1* **(a)**, *VvPIP1;2* **(b)**, *VvPIP2;1* **(c)** and  
819 *VvPIP2;4N* **(d)** transcripts. *Ubiquitin* (*VvUBI*) and *Actin1* (*VvACT1*) were used as  
820 endogenous control genes for the normalisation procedure. IRR, irrigated control; WS,  
821 water stress; RWS, recovery from water stress; PC, pressure collar stress; RPC,

822 recovery from pressure collar stress. Lower case letters denote significant differences ( $P$   
823  $< 0.05$ ) attested by using the Tukey's test, bars are standard errors of the mean ( $n = 3$ ).  
824  
825

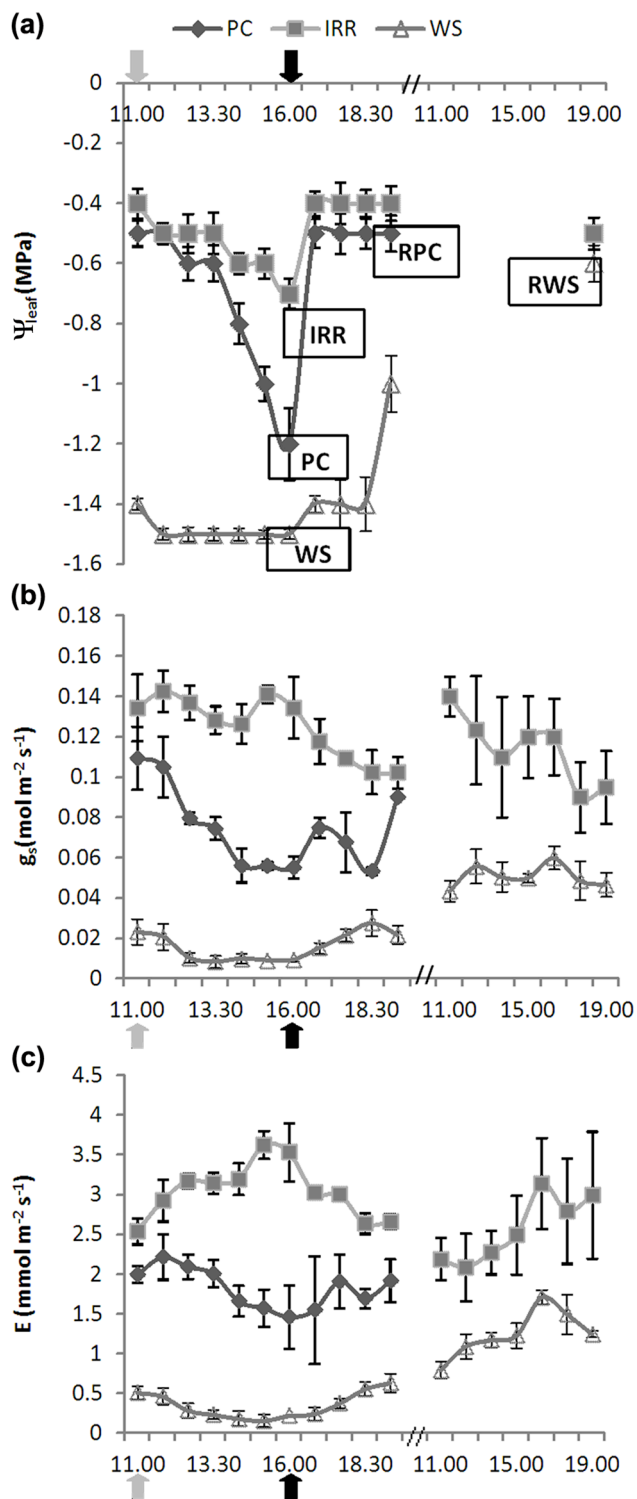


826

827

828 Fig 1

829

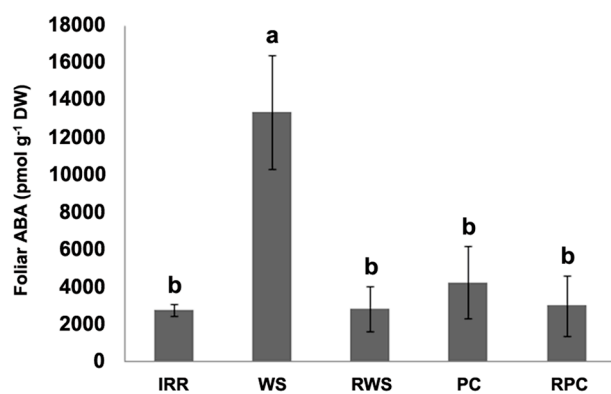


830

831 Fig 2

832

833



834

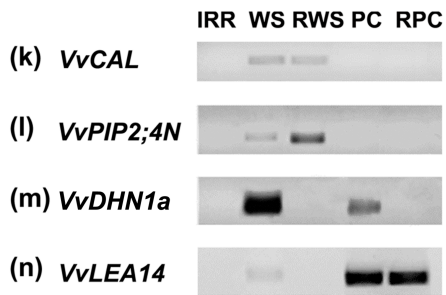
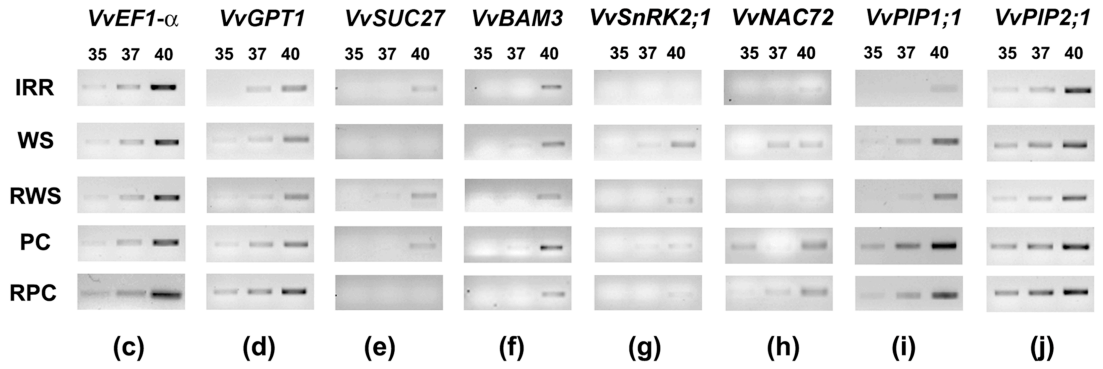
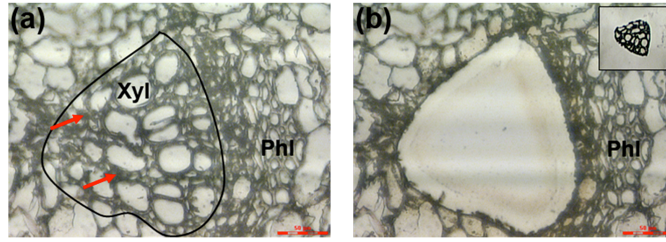
835 Fig 3

836

837

838

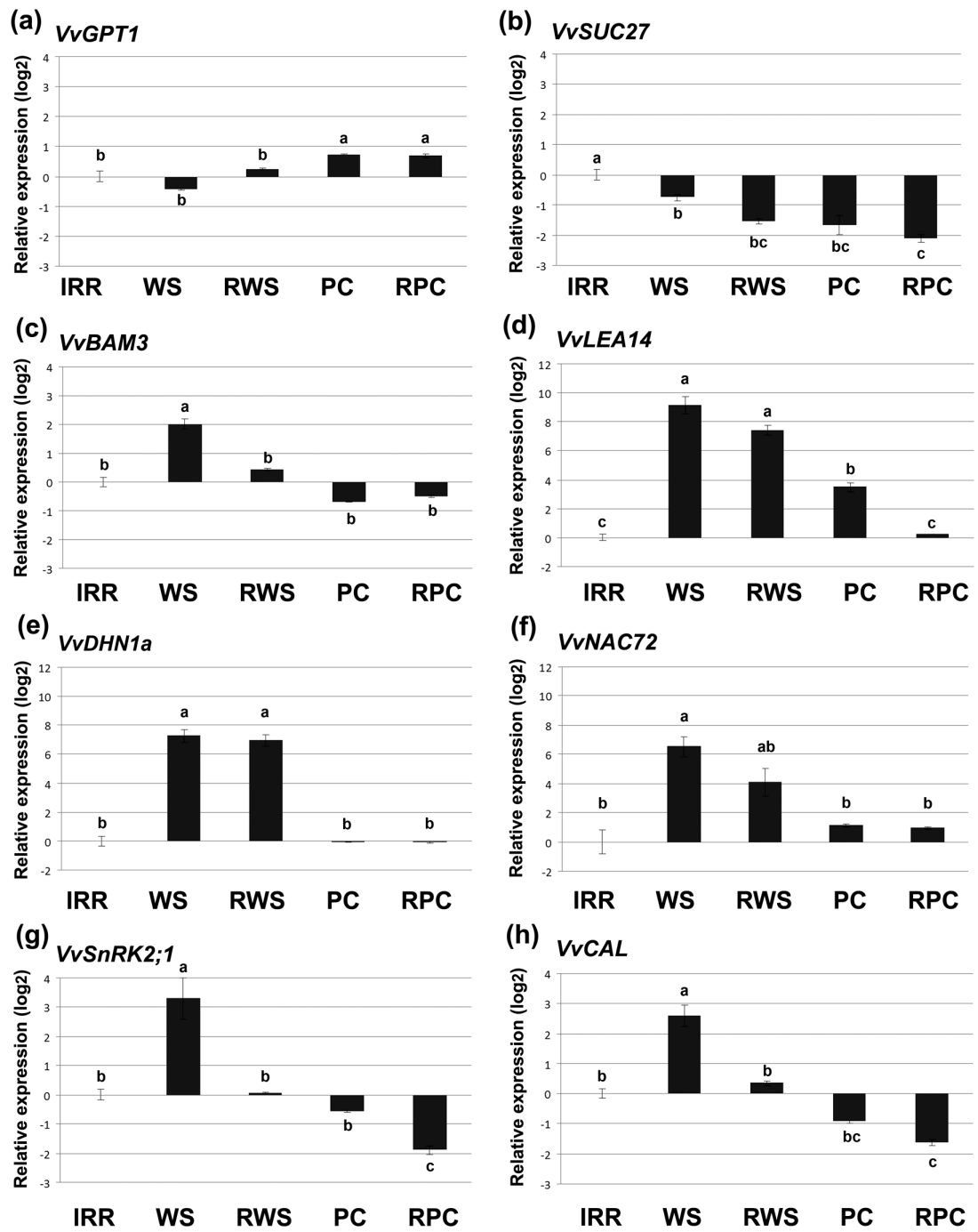




839

840 Fig 4

841

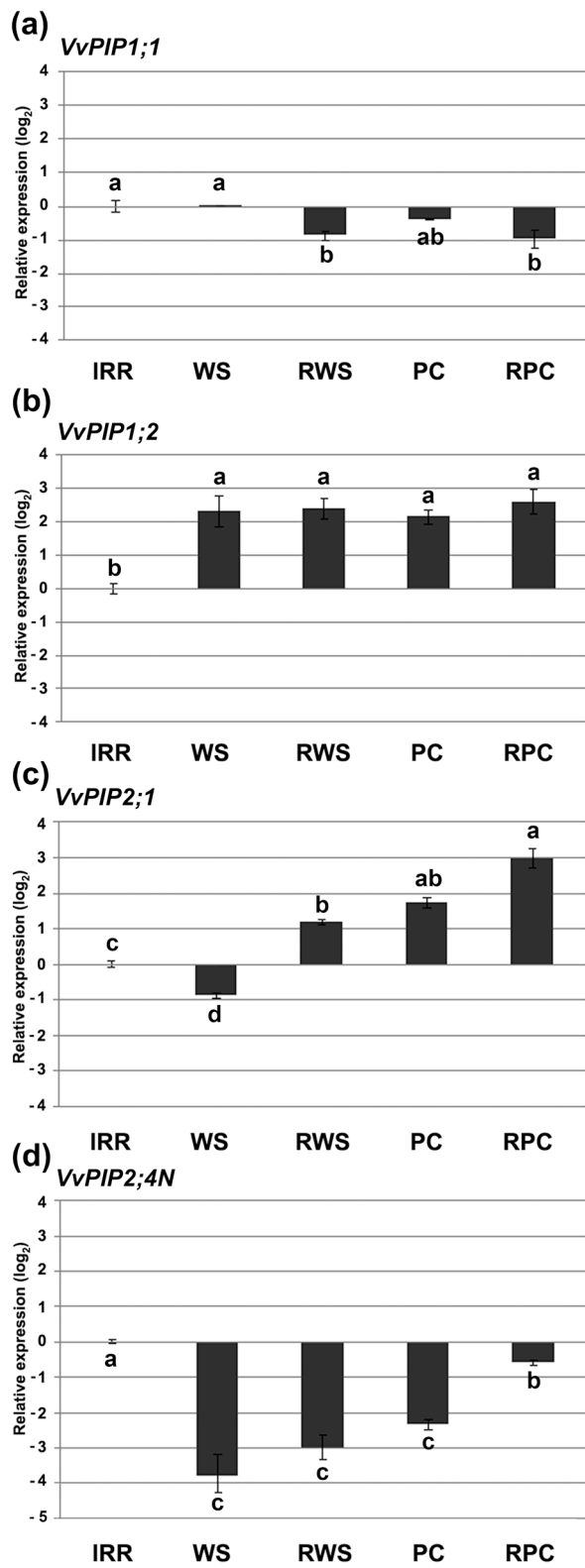


842

843 Fig 5

844

845



846

847

848 Fig 6

849

850 **Supplementary material captions**

851

852 **Supplementary Table S1** Oligonucleotides used in RT-PCR and semi-quantitative RT-  
853 PCR on LMD samples, and in RT-qPCR on whole petiole samples

854

855 **Supplementary Fig. S1** RT-PCR analysis on micro-dissected samples using primers  
856 for *VvEF1- $\alpha$*  gene as endogenous control gene. Any amplified product in RT-reactions  
857 excludes DNA contaminations. IRR, irrigated control; WS, water stress; RWS, recovery  
858 from water stress; PC, pressure collar stress; RPC, recovery from pressure collar stress

859

860 **Supplementary material**

861

862 **Table S1** Oligonucleotides used in RT-PCR and semi-quantitative RT-PCR on LMD samples, and  
 863 in RT-qPCR on whole petiole samples

Gene description	Gene ID (VVGDB 12X) and References	Primer	Primer sequences 5'-3'
<i>Actin 1 (VvACT1)</i>	VIT_04s0044g00580	Forward	GCCCCTCGTCTGTGACAATG
	Perrone <i>et al.</i> , 2012b	Reverse	CCTTGCCGACCCACAATA
<i>Ubiquitin (VvUBI)</i>	VIT_16s0098g01190	Forward	TCTGAGGCTTCGTGGTGGTA
	Perrone <i>et al.</i> , 2012b	Reverse	AGGCGTGCATAACATTTGCG
<i>Elongation factor 1-alpha (VvEF1-<math>\alpha</math>)</i>	VIT_06s0004g03240	Forward	GAAGTGGGTGCTTGATAGGC
	Reid <i>et al.</i> , 2006	Reverse	AACCAAAATATCCGGAGTAAAAGA
<i>Dehydrin 1a (VvDHN1a)</i>	VIT_04s0023g02480	Forward	AACCCGGCGTGCTTCAT
	Perrone <i>et al.</i> , 2012b	Reverse	CATGCCCGGTATCCTCTCTTT
<i>Late Embryogenesis Abundant Protein 14 (VvLEA14)</i>	VIT_15s0046g02110	Forward	CGTACAACGCCAAGGTCTCA
	Perrone <i>et al.</i> , 2012b	Reverse	CATCTTCCCGACGCTATCA
<i>NAC domain-containing protein 72-like (VvNAC72)</i>	VIT_19s0014g03290	Forward	CGCCCTCCAATCTTCTTCTCT
	Perrone <i>et al.</i> , 2012b	Reverse	AGCTGTGAAAGCGGGTCAGT
<i>Serine threonine kinase 2.1 (VvSnRK2;1)</i>	VIT_02s0236g00130	Forward	AGATGTTTGGTCTTGTGGTGTGA
	Perrone <i>et al.</i> , 2012b	Reverse	CCCAATGGTCTTCCGGAAT
<i>Calmodulin-like protein (VvCAL)</i>	VIT_15s0048g00790	Forward	TGGTCAGAGAAGTGGACTGCAA
	Perrone <i>et al.</i> , 2012b	Reverse	CAGGTGCTGCTGCTACCAACT
<i>Beta amylase (VvBAM3)</i>	VIT_02s0012g00170	Forward	CTAGCAGCTGCCGAAGGAAT
	Perrone <i>et al.</i> , 2012b	Reverse	CAGCCGCATGAGACCTTGTT
<i>Glucose-6-phosphate transporter</i>	VIT_10s0116g00760	Forward	TTCCGGTGCCGGTCTACTT

<i>(VvGPT1)</i>	Perrone <i>et al.</i> , 2012b	Reverse	GCCCCATAAACCCAGTCAT
<i>Sucrose transporter (VvSUC27)</i>	VIT_18s0076g00250	Forward	TGACCCCCTACGTTGAGCTT
	Perrone <i>et al.</i> , 2012b	Reverse	CCAACCTACCGGCTGCACAAT
<i>Aquaporin PIP1;1 (VvPIP 1;1)</i>	VIT_13s0067g00220	Forward	GAGTGGTGCTGGGCGTTGATC
	Choat <i>et al.</i> , 2009	Reverse	GTGGAATGCTACAGACATTAC
<i>Aquaporin PIP1;2 (VvPIP 1;2)</i>	VIT_15s0046g02420	Forward	TCCTCCATTTTCGTTTCTTC
	Choat <i>et al.</i> , 2009	Reverse	ATTGTAATAGAAGCAGCCCAG
<i>Aquaporin PIP2;1 (VvPIP 2;1)</i>	VIT_13s0019g04280	Forward	CCATTTTGATACCTTCTTCC
	Choat <i>et al.</i> , 2009	Reverse	TATCTACAATTCATGCCCTC
<i>Aquaporin PIP2;4N (VvPIP 2;4N)</i>	VIT_06s0004g02850	Forward	CTAGGATCTTTCAGGAGCAA
	Perrone <i>et al.</i> , 2012a	Reverse	TACTCCTCCACCATTGATGT

---

864

865

866

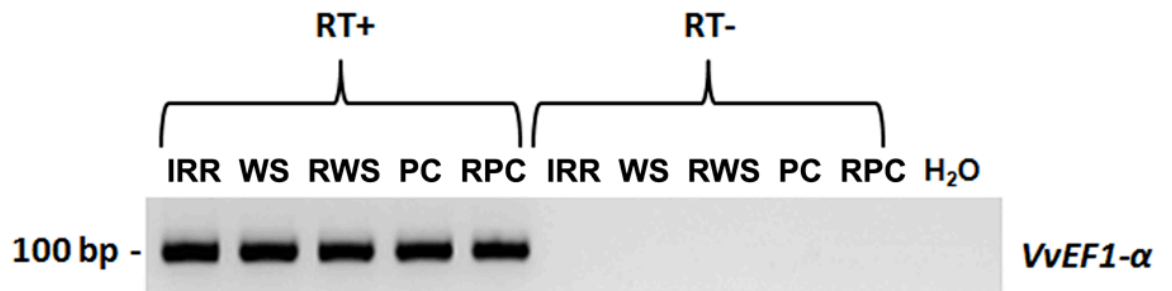
867

868

869 **Fig. S1** RT-PCR analysis on microdissected samples using primers for *VvEF1-α* gene, as  
870 housekeeping gene. Any amplified product in RT- reactions excludes DNA contaminations. IRR,  
871 irrigated control; WS, water stress; RWS, recovery from water stress; PC, pressure collar stress;  
872 RPC, recovery from pressure collar stress.

873

874



875

876

877

878